Partial oxidation of methanol on well-ordered V_2O_5(001)/Au(111) thin films

J. M. Sturm,† D. Göbke, H. Kuhlenbeck,*‡ J. Döbler,§ U. Reinhardt,‡ M. V. Ganduglia-Pirovano,‡ J. Sauer‡ and H.-J. Freund

Received 15th December 2008, Accepted 17th February 2009
First published as an Advance Article on the web 11th March 2009
DOI: 10.1039/b822384j

The partial oxidation of methanol to formaldehyde on well-ordered thin V_2O_5(001) films supported on Au(111) was studied. Temperature-programmed desorption shows that bulk-terminated surfaces are not reactive, whereas reduced surfaces produce formaldehyde. Formaldehyde desorption occurs between 400 K and 550 K, without evidence for reaction products other than formaldehyde and water. Scanning tunnelling microscopy shows that methanol forms methoxy groups on vanadyl oxygen vacancies. If methanol is adsorbed at low temperature, the available adsorption sites are only partly covered with methoxy groups after warming up to room temperature, whereas prolonged methanol dosing at room temperature leads to full coverage. In order to explain these findings we present a model that essentially comprises recombination of methoxy and hydrogen to methanol in competition with the reaction of two surface hydroxyl groups to form water.

1. Introduction

The partial oxidation of methanol to formaldehyde is regarded as a prototype reaction for the oxidative dehydrogenation of organic molecules. Vanadium oxides, often supported on other oxides, form an important class of catalysts for partial oxidation reactions.[1,2] The activity of vanadia oxidation catalysts is strongly dependent on the metal oxide support.[1,3] Since supported oxides are complex systems, detailed understanding of the reaction processes and atomistic mechanisms on these systems is hard to achieve. Studies of simpler systems, such as vanadium oxide single crystals or well-ordered thin films can help to elucidate some of these aspects. Previous studies in this direction include methanol adsorption on sub-monolayer to multilayer vanadia layers on TiO_2(110)[4,5] and CeO_2(111).[6,7] For vanadia on TiO_2(110) it was shown that (sub)-monolayers of vanadia are active, whereas multilayers of vanadia are inactive.[5] This was attributed to the involvement of M–O–V bonds (where M denotes the metal atom of the supporting metal oxide) in the partial oxidation reaction. Theoretical studies for the conversion of methanol to formaldehyde are presented in ref. 8 and 9.

A frequently found intermediate is methoxy, which is produced *via* fission of the OH bond of the methanol molecules resulting in methoxy groups and hydrogen atoms.[3,5] The final step for the formation of formaldehyde is hydrogen abstraction from the surface methoxy groups which occurs at elevated temperature. Thus, two hydrogen atoms are abstracted from the methanol molecule in the course of the formaldehyde production. These may react to form water, which leads to a net reaction $CH_3OH + O \rightarrow CH_2O + H_2O$. Since this reaction consumes oxygen, the oxidic substrate will be reduced if oxygen is not replenished from the gas phase.

Recently, we have shown that well-ordered V_2O_5(001) films can be grown on Au(111).[10,11] In this paper we present results of an investigation of the reactivity of nearly defect free and slightly oxygen-deficient V_2O_5(001) surfaces towards methanol oxidation. Reduced surfaces were prepared by electron irradiation, which mainly removes vanadyl oxygen atoms and results in preferential reduction of the surface. Reduction by thermal annealing was not used in the current case since defects tend to agglomerate upon annealing and a quantitatively well defined degree of reduction is harder to achieve. Furthermore, annealing leads to migration of oxygen to the surface, such that the bulk will become more reduced than the surface.[11,12] The effect of reduction by annealing is described in ref. 13 for a V_2O_5(001) single crystal surface and in ref. 11 for V_2O_5(001) on Au(111). The adsorption of methanol was studied with scanning tunnelling microscopy (STM), X-ray photoelectron spectroscopy (XPS) performed with the aid of synchrotron radiation and temperature-programmed desorption (TPD).

This paper is organised as follows: after a description of the experimental and theoretical details in section 2, the results are presented and discussed in section 3. Based on a combination of results from the different techniques that were employed, an adsorption model is developed which is presented and compared with experimental results and theory in sections 3.5 and 3.6. Conclusions follow in section 4.

2. Experimental and theoretical details

Oxide film preparation, STM measurements and TPD experiments were carried out in an ultra-high vacuum (UHV) system

Fritz Haber Institute of the Max Planck Society, Chemical Physics Department, Faradayweg 4-6, 14195 Berlin, Germany
† Present address: FOM-Institute for Plasma Physics Rijnhuizen, Postbus 1207, 3430 BE Nieuwegein, The Netherlands.
‡ Humbold-Universität zu Berlin, Department of Chemistry, Unter den Linden 6, 10099 Berlin, Germany.
§ Present address: Humbold-Universität zu Berlin, Computer and Media Services, Unter den Linden 6, 10099 Berlin, Germany.

with a base pressure below 1×10^{-10} mbar. This system incorporates a commercially available STM[14,15] in which etched tungsten tips were used. TPD experiments were carried out with a differentially pumped quadrupole mass spectrometer (QMS)[16] equipped with a Feulner cup,[17] in order to reduce the influence of the background pressure on the spectra. For all spectra, a heating rate of 0.5 K s^{-1} was used. Methanol (CH_3OH, pro analysis, Merck) was cleaned by numerous freeze–pump–thaw cycles and dosed onto the surface with a gas doser that preferentially exposes the sample surface to gases, thereby maintaining a low background pressure in the UHV system. High-resolution XPS spectra were measured with a Scienta R4000 electron energy analyser in a UHV chamber connected to the UE52-PGM beam line of the synchrotron radiation facility BESSY (Berlin, Germany). The preparation and characterisation of the $V_2O_5(001)$ films has been described in recent publications.[10,11] Metallic vanadium was evaporated onto a clean Au(111) single crystal, followed by oxidation in 50 mbar O_2 at 670 K for 10 min. TPD and XPS results shown here are exclusively from experiments carried out using films grown by three cycles of deposition of 6 Å vanadium followed by oxidation. This procedure reproducibly forms closed films of well-ordered $V_2O_5(001)$ crystallites.[11] Controlled reduction of the oxide films was realised by electron bombardment with a hot filament facing the sample surface. The electron energy was set to 50 eV by applying a bias voltage to the sample.

Calculations are based on spin DFT and employ a plane wave basis set (400 eV cutoff) as implemented in the VASP code with the PBE functional.[18] The defective (3×1) $V_2O_5(001)$ surface was modelled using a two-layer slab and a $(2 \times 2 \times 1)$ k-mesh.

3. Results and discussion

3.1 Temperature-programmed desorption

Fig. 1 shows a TPD spectrum of methanol on an as-prepared, nearly defect-free bulk-terminated V_2O_5 film. Only molecular methanol was found in the desorbing products. The most intense peaks in the cracking pattern of methanol are masses 29 and 31, which have an intensity ratio of about 2 to 1. The absence of desorbing gases other than methanol indicates that the defect-free surface is not active for reactions of methanol. Reactive surfaces can be obtained by removing vanadyl oxygen with the aid of electron irradiation. On films reduced in this way formaldehyde is produced, as indicated by the presence of a desorption signal in the mass 29 spectrum (29 is the most abundant mass in the mass cracking pattern of formaldehyde[19]) without corresponding intensity at mass 31. Fig. 2 compares TPD spectra (mass 29) obtained after dosing 5 L of CH_3OH at 100 K (1 L = 1.33×10^{-6} mbar s) onto surfaces reduced with different electron doses. For low electron doses, formaldehyde desorption takes place at about 510 K, whereas for an electron dose of 3 mC an additional broad desorption peak centred around 450 K arises, which dominates for doses of 5 mC and more. According to STM results (not shown here) the vanadyl double rows (as present on regular $V_2O_5(001)$) can hardly be recognised any more for this electron dose. For all TPD spectra the

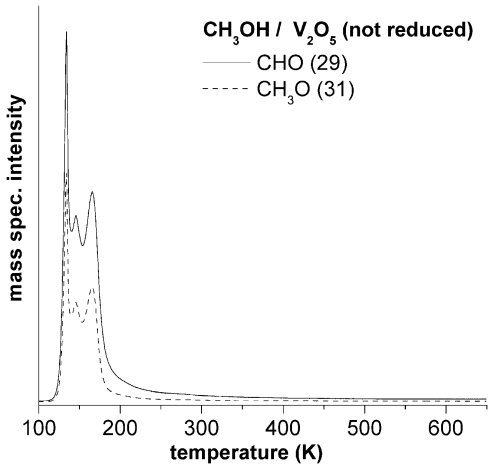

Fig. 1 TPD spectrum of 5 L methanol dosed at 100 K on non-reduced V_2O_5. The solid line represents mass 29 and the dashed line mass 31.

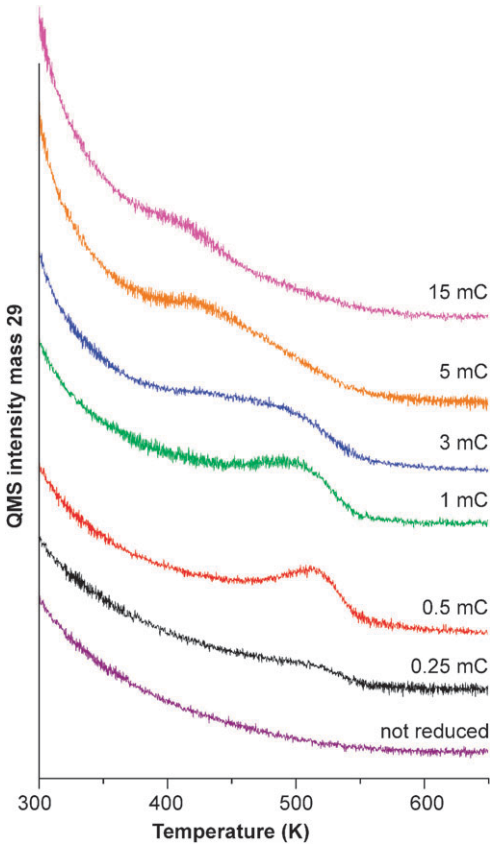

Fig. 2 TPD spectra (mass 29, indicating formaldehyde) of 5 L methanol adsorbed at 100 K on V_2O_5 reduced with various electron doses. The electron doses employed for reduction are indicated in mC.

masses corresponding to H_2, H_2O, CO, CO_2 and CH_4 were also recorded, but no evidence for the desorption of species other than methanol, formaldehyde and water was found. In addition, STM images recorded after TPD did not show any structures indicative of the presence of species remaining on the surface. The absence of detectable CO and CO_2 amounts indicates that formate formation did not take place since CO

and CO_2 are common formate combustion products. The temperature window for formaldehyde desorption is similar to that found for well-ordered $V_2O_3(0001)$ films on Au(111)[20] and supported vanadium oxide layers and clusters,[4–7,21] which may be related to similar mechanisms for hydrogen abstraction. Our finding that non-reduced, vanadyl-terminated films are not reactive for methanol oxidation is in line with previous results for non-reduced V_2O_3 films that are also terminated with vanadyl groups.[11] Furthermore, also non-reduced multilayers of vanadium oxide on $TiO_2(110)$ were found to be not reactive.[5]

3.2 STM statistics

Fig. 3(a) shows a STM image of a $V_2O_5(001)$ film, which was reduced by exposure to an electron dose of 3 mC. Missing vanadyl oxygen atoms are imaged as depressions (dark colour) as discussed in ref. 11. These defects, created by electron bombardment, act as adsorption sites for methoxy groups, visible as bright blobs after exposure to methanol (b). The STM images show that not all defects are covered. A flash to 560 K removes the methoxy groups and image (c) is observed. The density of surface defects is reduced to about 0.6 times the defect density after reduction (a) and a large fraction of the remaining defects have coalesced. These effects are probably mainly caused by migration of oxygen from deeper layers to the surface at elevated temperature[11,12] and defect migration in the surface plane. Because of this, it is not possible to investigate whether the formaldehyde production leaves additional defects in the V_2O_5 layer due to oxygen consumption. In Fig. 4, we summarise an analysis of the number of defects after reduction and the number of methoxy groups and remaining defects after subsequent methanol exposure, as obtained from

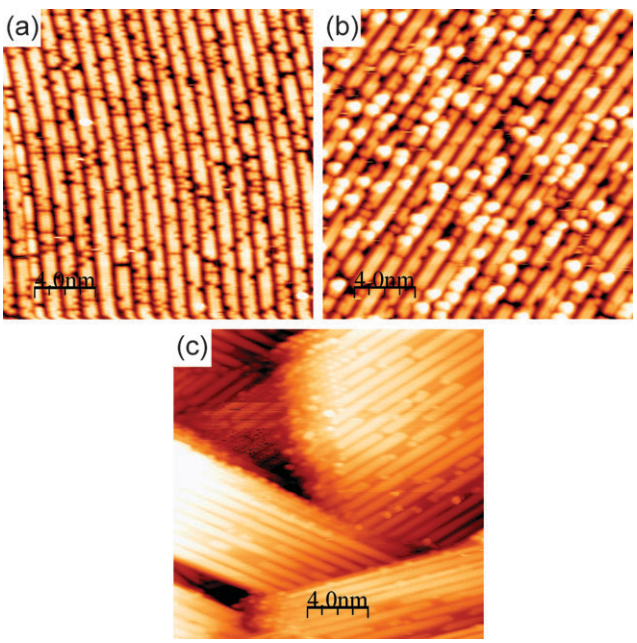

Fig. 3 STM images of a V_2O_5 film: (a) after reduction with 3 mC of electrons; (b) after subsequent exposure to 10 L CH_3OH at room temperature; (c) after flashing to 560 K. The imaged area is 20 × 20 nm in all cases. The images were acquired in constant current mode with a tunnelling current of 0.2 nA and bias 2.0 V (a) or 2.5 V (b–c).

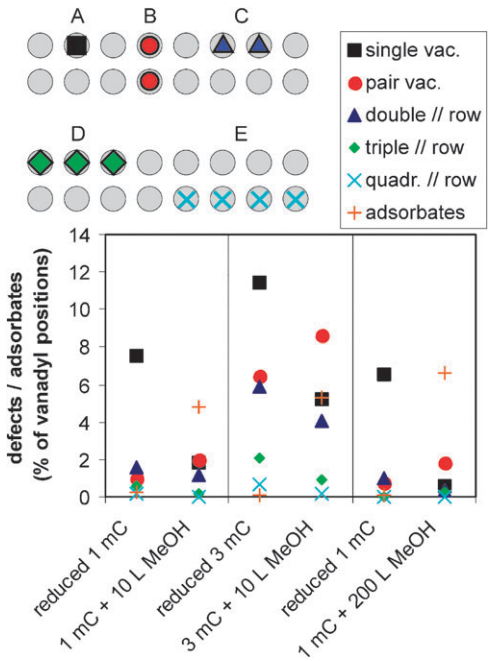

Fig. 4 STM statistics of defects (oxygen vacancies) after reduction and remaining defects and methoxy adsorbates (symbol +) after methanol exposure at room temperature. The coverage is expressed as percentage of the amount of vanadyl lattice sites in the analysed area. The legend key is explained in the drawing, where grey spheres indicate vanadyl lattice sites.

STM data. For each stage, at least 3 STM images of different areas on the sample were analysed and the number of defects and adsorbates is expressed as percentage of the number of vanadyl sites on a non-reduced surface. Different types of defects were distinguished (labelled with characters A–E, see Fig. 4), namely single (isolated) vanadyl oxygen vacancies (A), vanadyl pair vacancies (two oxygen atoms of a vanadyl pair perpendicular to a vanadyl double row both removed, B) and multiple vacancies along a row (C–E). Fig. 4 shows that the density of all types of defects except type B decreases upon methanol adsorption. The decrease is easily understood in view of the formation of surface methoxy groups but for the increase of the number of type B defects another mechanism must be responsible, which will be discussed at a later point. The STM analysis also shows that for a methanol dose of 10 L the reactive vacancies are only partially covered.

The data displayed in Fig. 4 have been obtained from moderately reduced surfaces where the vanadyl double rows are still easily recognisable. Fig. 2 shows that the formaldehyde production drops rapidly if the electron dose is increased further so that the maximum amount of formaldehyde formed on $V_2O_5(001)$ films is smaller by about an order of magnitude than the amount formed on $V_2O_3(0001)$ films.[20] We can only speculate what the reasons for this result could be. The STM results suggest that B type defects cannot chemisorb methoxy. Since larger electron doses produce more B type defects, this can partly explain the decrease in reactivity. As has been shown for $V_2O_5(001)$ single crystals[13] and thin films,[11] reduction may lead to $V_6O_{13}(001)$ type structures. We did not yet investigate the reactivity of $V_6O_{13}(001)$ towards

methanol oxidation but it may well be the case that this type of surface in inactive.

3.3 Synchrotron XPS

One could imagine two reasons for the partial coverage of the reactive oxygen vacancies. First, it might be that two types of isolated defects exist that are indistinguishable in STM but of which only one can chemisorb methoxy. A second explanation is that a part of the methoxy groups can recombine with hydroxyl groups below room temperature, forming molecular methanol that leaves the surface. This will also result in a partial coverage of the defects at room temperature as observed in the STM experiments. The TPD spectra of methanol on reduced V_2O_5 indeed show a methanol peak in the temperature range 230 K to 300 K (see Fig. 5, black lines, label "LT"), which could result from such a recombination process. XPS was utilised to show that the methanol desorption peak can in fact be attributed to a recombination reaction and not to desorption of molecularly adsorbed methanol. Fig. 6 shows a set of C 1s spectra recorded at 100 K sample temperature under highly surface sensitive conditions: the photoelectron take off angle was set to 70° with respect to the surface normal and the photon energy was set to 380 eV. The latter value gives a kinetic energy of the C 1s electrons of about 100 eV, which is an energy where the inelastic mean free path length is small. The as-prepared film shows a C 1s peak at 283.8 eV, which is related to a carbon contamination of the film. This contamination is due to carbon incorporation into the film occurring during the evaporation of metallic vanadium onto the substrate which is the first step of the oxide film preparation. The metallic vanadium may dissociate CO molecules from the residual gas atmosphere, which would contaminate the thickening film with carbon.

After reduction and methanol adsorption, the sample was flashed to 230 K in order to desorb the molecularly adsorbed methanol. In the corresponding C 1s spectrum a large peak at 286.2 eV binding energy is found, which is attributed to methoxy groups. A smaller contribution of molecular

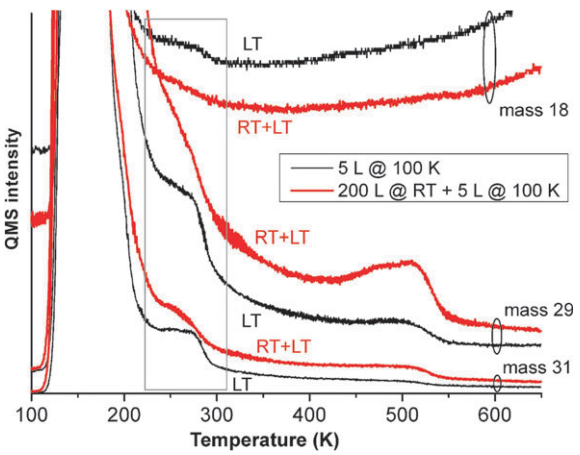

Fig. 5 TPD spectrum of methanol on V_2O_5 reduced with an electron dose of 1 mC; black lines (label "LT") correspond to 5 L methanol dosed at 100 K and red lines (label "RT + LT") correspond to 200 L methanol dosed at RT plus 5 L at 100 K.

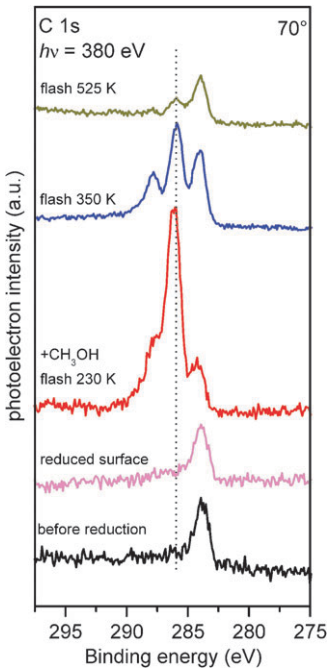

Fig. 6 XPS C 1s spectra measured at 100 K using synchrotron radiation with a photon energy of 380 eV. From bottom-to-top the curves represent the situation before reduction, after reduction, after subsequent methanol exposure at 100 K and flashing to 230 K, 350 K and 525 K, respectively. The dotted line indicates the binding energy of methoxy: 286.2 eV.

methanol at 288.0 eV is also found which we assign at least partly to be due to adsorption of methanol from the residual gas atmosphere (for methanol on $V_2O_3(0001)$[20] and $CeO_2(111)$[26] binding energies also near to 288 eV were found). In the XPS chamber a less effective dosing system was used, therefore a slight contamination of the residual gas atmosphere with methanol could not be avoided.

The binding energies found for methoxy and methanol compare well to other reports in the literature[22–26] with the remark that the reported binding energies vary somewhat depending on the substrate (see ref. 26 and references therein). Flashing to 350 K clearly results in a loss of methoxy, whereas the amount of molecular methanol remains approximately constant. After flashing to 525 K most of the methoxy has left the surface to produce formaldehyde. Thus, the XPS results clearly show that the methanol desorption peak between 230 K to 300 K in Fig. 5 is due to a recombination of methoxy and hydroxyl groups to methanol followed by desorption. This process frees part of the defects covered with methoxy groups and leads to the observed partial coverage at room temperature. Based on these results we exclude that two types of single defects exist, of which only one type is reactive. Of course, this discussion currently leaves open the question why only a part and not all of the methoxy groups transform into methanol *via* recombination with hydrogen from the hydroxyl groups. This issue will be discussed in the following.

3.4 Methanol adsorption at room temperature

Nearly full methoxy coverage of the reactive oxygen vacancies can be achieved by dosing a relatively large amount of

methanol at room temperature (RT). The right column in Fig. 4 shows that for a methanol dose of 200 L at RT practically all reactive defects are covered, whereas this is not the case for a dose of 10 L. The larger methoxy coverage obtained by a large dose at RT also results in the production of more formaldehyde, as shown in Fig. 7(a). For the TPD spectrum of 5 L methanol dosed at 100 K, the surface was reduced at RT and cooled to 100 K, followed by methanol dosing. Subsequently the TPD experiment was started. For the spectra with a 200 L dose at RT, the surface was also reduced at RT, followed by the exposure to 200 L methanol. Subsequently the sample was cooled to 100 K and an additional exposure to 5 L methanol was performed. This procedure guarantees that the TPD spectra have similar backgrounds (resulting from the desorption of the methanol multilayer) such that the data can easily be compared. Fig. 7(a) shows clearly that a dose of 200 L methanol at RT, leading to a nearly full coverage of the reactive defects according to STM, results in a 2 to 3 times larger formaldehyde yield than a dose of 5 L at 100 K. This factor favourably compares to the XPS data of Fig. 6, which show that the methoxy coverage after flashing to 230 K is ~2 times larger than the methoxy coverage after flashing to 350 K. This indicates that up to 230 K the available adsorption sites are nearly fully covered with methoxy groups.

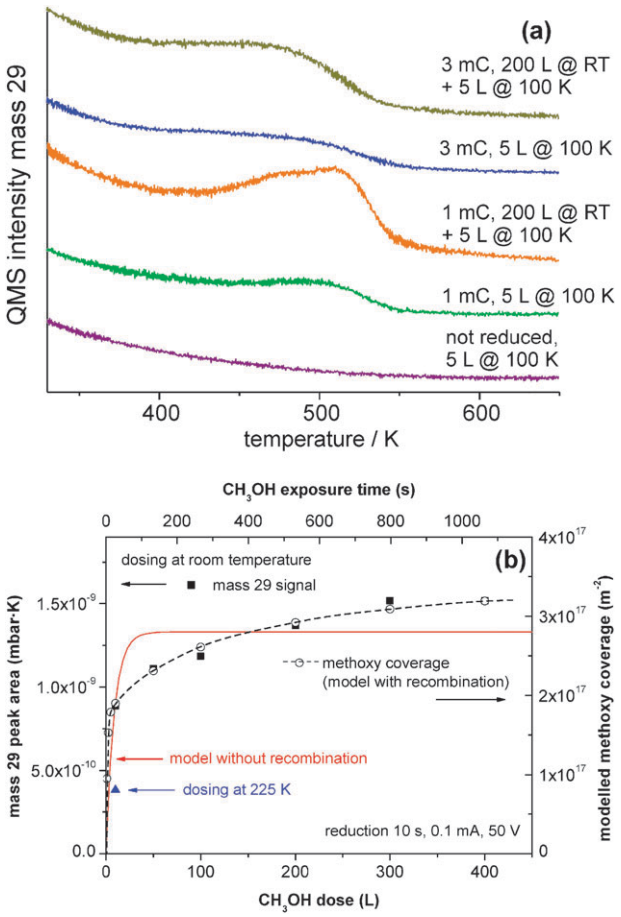

Fig. 7 (a) TPD plots (mass 29) of methanol on different $V_2O_5(001)$ surfaces, parameters are given in the plot. The electron dose used for surface reduction is given in mC followed by methanol dose and dosing temperature. (b) TPD formaldehyde peak area *versus* methanol dose at room temperature (solid squares) and formaldehyde peak area for 10 L methanol at 225 K (triangle). The surface was reduced with an electron dose of 1 mC for all data points. The solid (red) line indicates the best fit to the RT data assuming a sticking coefficient that is proportional to the number of free adsorption sites and ignoring methanol–hydroxyl recombination. The open circles (connected with a dashed line to guide the eye) indicate the modelled methoxy coverage using a model that includes simultaneous recombination of methoxy and OH towards methanol and combination of OH to form water.

Fig. 7(b) (square solid markers) shows the formaldehyde production as a function of the methanol dose at room temperature for a surface reduced with an electron dose of 1 mC. The methanol dose was varied by means of the exposure time, with a fixed dosing rate of 0.38 L s^{-1}. The dependence shows that the limited coverage for lower doses cannot simply be the result of a sticking coefficient below unity, but results from a more complex adsorption process: already for low doses a significant coverage is reached, whereas a further increase in the coverage only proceeds very slowly with increasing dose. The solid (red) line in the plot represents the best fit of the formaldehyde yield *versus* dose that could be obtained for the case of a sticking coefficient proportional to the number of free adsorption sites. It is obvious that the experimental behaviour cannot be explained when only a coverage-dependent sticking coefficient is taken into account.

3.5 Model for methanol adsorption on $V_2O_5(001)$

We explain the observed adsorption behaviour at RT in terms of the suggested methoxy-hydroxyl recombination. When a methanol molecule adsorbs on a defect, it forms a methoxy and a hydroxyl group, similar to the situation on $V_2O_3(0001)$.[8]

$$V + VO + CH_3OH \rightarrow CH_3OV + VOH \qquad (1)$$

where V denotes a defect site, VO a vanadyl group, VOH a hydroxyl group and CH_3OV a methoxy group. Parts of the methoxy and hydroxyl groups recombine, forming molecular methanol, which can desorb from the surface and leave uncovered defects. This is in agreement with results of Burcham and Wachs[27] who reported that the dissociative chemisorption of methanol on supported V_2O_5 is reversible. However, it is obvious that the adsorption process in the current case is not fully reversible since a part of the methoxy groups stays on the surface even at room temperature and forms formaldehyde upon further heating to ~500 K. The question to be discussed now is which factor determines the number of methoxy groups staying on the surface and the number, which forms methanol with hydrogen from the hydroxyl groups. This factor is probably the number of hydroxyl groups on the surface. These can react with methoxy groups to form methanol but they can also react with other hydroxyl groups to form water. If the latter process occurs, the number of hydroxyl groups on the surface will become smaller than the number of methoxy groups. As a result, not all methoxy groups can react with hydrogen to form methanol and a part stays on the surface, finally being transformed into formaldehyde at elevated temperature. In the following, we will put together arguments substantiating this assumption.

It has already been discussed that low temperature adsorption of methanol leads to a partial coverage of the available adsorption sites after annealing up to room temperature. This agrees well with the model presented above if we assume that the water is formed during warming up at some temperature below room temperature *via* a combination reaction of a part of the hydroxyl groups. Another part of the hydroxyl groups reacts with methoxy groups, forming methanol. Both processes produce uncovered adsorption sites according to:

$$\mathrm{VOH} + \mathrm{VOH} \rightarrow \mathrm{VO} + \mathrm{V} + \mathrm{H_2O}\ (\text{water formation}) \quad (2)$$

$$\mathrm{VOH} + \mathrm{CH_3OV} \rightarrow \mathrm{VO} + \mathrm{V} + \mathrm{CH_3OH}\ (\text{methanol formation}) \quad (3)$$

Assuming that molecularly adsorbed methanol is not available to react with free adsorption sites at the temperature where these reactions occur, uncovered adsorption sites as well as methoxy groups are to be expected at RT, which is in agreement with the STM observations. The TDS data presented in Fig. 5 show that methanol formation occurs between 230 K and 300 K, which is supported by the XPS data shown in Fig. 6. There is no equally clear evidence for the formation of water. TPD spectra of water on reduced V_2O_5 (not shown here) suggest that a part of the hydroxyl groups formed by water dissociation on defects combines to form water below room temperature, whereas another part stays on the surface up to 425 K. The latter observation is supported by room temperature STM experiments, since the hydroxyl groups that are stable up to RT could be imaged. Studies of water adsorption on reduced V_2O_3(0001) give a similar result in that water formation *via* reaction of hydroxyl groups was observed below room temperature but also desorption states above room temperature were found.[28] In the case of methanol adsorbed on reduced V_2O_3(0001) at low temperature, the reaction of hydroxyl groups to form water could clearly be detected at $\sim$250 K.[20] No evidence for the presence of hydroxyl groups on methoxy covered V_2O_5(001) surfaces was found with STM, which supports our suggestion that all or most hydroxyl groups combine below room temperature. However, we note that hydroxyl cannot easily be identified because of the small height contrast of a hydroxyl group (typically 0.2 Å) relative to a methoxy group (typically 1.5 Å). Also in the XPS experiments the hydroxyls could not be observed. This is probably related to the low coverage, in combination with the relatively small difference in binding energy between oxygen in hydroxyl (531.3 eV, according to[28] and oxygen in V_2O_5 (529.9 eV). A weak signature of water formation below room temperature is found in the TPD spectrum of 5 L methanol on mildly reduced V_2O_5 (black lines, label "LT" in Fig. 5) which shows a tiny peak in the mass 18 signal in the temperature range between 230 K and RT. We note, however, that this observation is not an irrefutable proof of water formation on the surface, since in this temperature range also methanol desorption occurs. TPD spectra of molecular methanol always show a mass 18 signal when methanol (mass 29 and 31) is detected, which is presumably due to an exchange reaction at the walls of the mass spectrometer housing.

The TPD and STM experiments show that the number of unoccupied defect sites decreases with increasing methanol exposure time at room temperature. This effect is due to the reaction of hydroxyl groups to form water and the recombination of methoxy and hydroxyl to form methanol while the surface is dosed with methanol. Thus, unoccupied defects produced by the water and methanol formation reactions can react again with methanol to form methoxy and hydroxyl. Since water desorbs but is not supplied from the gas phase this process leads to a decrease of the density of hydroxyl groups such that the hydroxyl coverage ultimately approaches zero for a large exposure time. As a result, the recombination reaction terminates and a full coverage of the reactive defects is achieved.

When 200 L methanol is dosed on the reduced surface at RT, followed by 5 L at 100 K, the methanol desorption signal between 230 K and RT almost completely vanishes, as shown by the red lines (label "RT + LT") in Fig. 5. This fits to our adsorption model: the large dose at RT covers practically all available adsorption sites with methoxy. Consequently, only the methanol peaks from molecularly adsorbed methanol are observed in the temperature range from 120 to 200 K, whereas the desorption signals of methanol (and possibly water) between 230 K and RT have almost completely vanished.

The reaction of hydroxyl groups to form water produces additional surface defects. This is probably the reason for the increase of the density of type B defects (vanadyl oxygen vacancy pairs perpendicular to the vanadyl double rows) after methanol dosing, as observed in the STM statistics results (Fig. 4). We assume that the reaction of two hydroxyl groups is facilitated near a single vacancy, such that a vanadyl pair vacancy remains after hydroxyl combination. Of course, this remains speculation without additional evidence.

3.6 Energy barriers for (re)combination reactions

We will now assess whether the model with simultaneous methoxy–hydroxyl recombination and hydroxyl–hydroxyl combination can explain the dependence of the formaldehyde production on the methanol dose at room temperature (Fig. 7(b)). The adsorption process can be described by a set of two differential equations for the change in methoxy coverage θ_M and OH coverage θ_{OH} with time t:

$$N_{tot}\frac{d\theta_M}{dt} = S(\theta)\cdot\Phi_M - N_{tot}\theta_M\theta_{OH}\nu\exp\left(-\frac{E_1}{kT}\right), \quad (4)$$

$$N_{tot}\frac{d\theta_{OH}}{dt} = S(\theta)\cdot\Phi_M - 2N_{tot}\theta_{OH}^2\nu\exp\left(-\frac{E_2}{kT}\right) - N_{tot}\theta_M\theta_{OH}\nu\exp\left(-\frac{E_1}{kT}\right), \quad (5)$$

where N_{tot} equals the number of vanadyl lattice sites (4.8×10^{18} m^{-2}), $S(\theta)$ a coverage-dependent sticking coefficient, Φ_M the flux of methanol molecules per unit area and time, ν the attempt frequency (10^{13} s^{-1}), E_1 and E_2 the energy barriers for methoxy–OH recombination and OH combination, respectively, k Boltzmann's constant and T the adsorption temperature (RT = 298 K). This model assumes that both reactions follow a unique reaction path and the effect of surface diffusion is neglected. In view of the low defect

density, diffusion surely plays a role but if this is much faster than the water and methanol formation reactions its influence will be negligible. We assume a coverage-dependent sticking coefficient of the form:

$$S(\theta) = \frac{N_0 - N_M}{N_{tot}}, \quad (6)$$

with N_0 the number of possible adsorption sites per unit area and N_M the number of methoxy groups per unit area ($N_M = \theta_M \cdot N_{tot}$). This equation assumes that methanol molecules that hit the surface at an unoccupied defect site do stick, whereas molecules that hit a non-reduced or occupied surface site do not react. However, the accurate expression for the sticking coefficient is not a critical ingredient for our experimental conditions, since the rate at which methanol molecules hit the surface is three orders of magnitude higher than the calculated desorption rate of water and methanol formation. In this case, the reactive defects are always nearly fully covered while methanol is dosed.

As the set of differential equations is non-linear, an analytical solution probably does not exist. Therefore, we numerically solved the equations using the Mathematica program package.[29] The calculation was broken up into two steps; the first one modelled the processes on the surface during the time while methanol was dosed and the second one modelled the reactions on the surface after the methanol supply from the gas phase was switched off. In the first step we calculated the methoxy and OH coverage *versus* time starting from zero coverage at $t = 0$. The value of N_0 was taken to be 7.5% of N_{tot}, according to the density of single (type A) defects on a surface reduced with an electron dose of 1 mC (see Fig. 4). Since also defect types C, D and E can adsorb methoxy, this value of N_0 is not fully correct. However, close inspection of the STM results shows that for a mild reduction with an electron dose of 1 mC about 90% of the methoxy coverage can be attributed to adsorption on single defects. If the calculations are performed with a higher density of defects in order to include row defects, the influence on the calculated adsorption behaviour is only in the order of 1%, a small error in view of the spread in the experimental data points. Furthermore it is not known if the energetics of the (re)combination reactions is equal for methoxy groups on single and multiple defects, such that the simplification is justified. The methanol flux from the gas phase Φ_M was set to 1.35×10^{18} molecules m^{-2} s^{-1} (dosing rate 0.38 L s^{-1}). The calculation was stopped when t reached the end of the dosing period. With the coverages obtained at the end of step 1 and Φ_M set to zero the second step was started. The calculation was stopped when the hydroxyl coverage θ_{OH} was near to zero. At this point the recombination reaction terminates and the stable methoxy coverage $\theta_{M,end}$ is found. This methoxy coverage corresponds to the methoxy groups that produce formaldehyde upon heating and can be compared to the measured formaldehyde signal for various methanol doses at RT. Such a comparison is presented in Fig. 7(b), where the open circles connected by the dashed line represent the modelled methoxy coverage $\theta_{M,end}$, for E_1 and E_2 equal to 0.85 eV per molecule. The agreement between the experimental data and the model is virtually perfect.

In our model, we only regard defects induced by the electron beam reduction as possible adsorption sites for methoxy groups. This approach ignores that the reaction of two hydroxyl groups to form water produces additional surface defects. For methanol adsorption on $V_2O_3(0001)$ it was unambiguously shown that the defects formed by water formation also adsorb methoxy groups, such that the maximum methoxy coverage that can be obtained equals twice the initial defect density.[20] The right column in Fig. 4 shows that this effect is not observed for $V_2O_5(001)$, since the number of methoxy groups that could be adsorbed with a dose of 200 L at room temperature is approximately equal to the number of defects created by e-beam reduction while not too many unoccupied isolated defects remain visible after methanol dosage. However, all three panels in Fig. 4 show that the number of unoccupied type B defects increases after exposure to methanol. We assume that single defects catalyse water formation, which would lead to double defects after water desorption. This process would not just render inactive the defects produced by water desorption but also those defects which catalysed water formation. On the other hand, we do not know whether the formation of isolated defects by water desorption can really be excluded. If this process does occur, the isolated defects produced this way could partly or fully counterbalance the loss of active defects due to formation of type B double defects.

Dosing 10 L methanol at temperatures below the temperature range where methoxy–OH recombination and hydroxyl–hydroxyl combination take place, results in a considerably lower formaldehyde yield compared to 10 L at room temperature (see triangle marker in Fig. 7). This indicates that dosing at low temperature followed by warming up leads to more methanol formation *via* methoxy–hydroxyl recombination and thus a smaller final methoxy coverage and a smaller formaldehyde yield than dosing at room temperature. A likely origin for this difference is the influence of diffusion. The room temperature STM images do not show any evidence that the methoxy species are mobile, so that it is safe to assume that at RT and below the surface methoxy groups do not diffuse. On the other hand, hydroxyl groups probably do diffuse on the surface since otherwise the formation of water *via* reaction of hydroxyl groups would not be explainable in view of the limited density of adsorption sites on the surface. The diffusing hydroxyl groups can either react with a methoxy group to form methanol or react with another hydroxyl group to form water. In the case of water formation both reaction partners diffuse on the surface, such that this reaction profits more from a faster surface diffusion at higher temperature than the formation of methanol. This is in agreement with the experimental findings: the larger mobility of hydroxyl groups at higher temperature results in a higher water formation rate, such that the hydroxyl coverage decreases more rapidly and a larger final methoxy coverage is achieved. There are other ingredients in this discussion, like the possible small separation of methoxy and hydroxyl after their formation from methanol. This could favour methoxy–OH combination at low temperature when hydroxyl diffusion is slow as well as different attempt frequencies for the water and methanol formation reactions.

In order to assess whether the calculated values of the energy barriers are correct, we have calculated water and methanol desorption spectra (for the reaction of hydroxyl groups to form water and the reaction of methoxy with hydroxyl groups to form methanol). In this way the energy barriers of these reaction can be extracted from the methanol desorption temperature ($\sim$275 K) found in the TPD spectra of Fig. 5. Since the methoxy–OH recombination, leading to methanol desorption and OH combination, leading to water desorption have to be taken into account simultaneously, the standard analysis of Redhead[30] cannot be directly used. To describe the current case we formulate differential equations for the change in methoxy and OH coverage with temperature T for a linear heating rate β:

$$\frac{\mathrm{d}\theta_{\mathrm{M}}}{\mathrm{d}T} = -\frac{\nu}{\beta}\theta_{\mathrm{M}}\theta_{\mathrm{OH}}\exp\left(-\frac{E_1}{kT}\right), \quad (7)$$

$$\frac{\mathrm{d}\theta_{\mathrm{OH}}}{\mathrm{d}T} = -2\frac{\nu}{\beta}\theta_{\mathrm{OH}}^2\exp\left(-\frac{E_2}{kT}\right) - \frac{\nu}{\beta}\theta_{\mathrm{M}}\theta_{\mathrm{OH}}\exp\left(-\frac{E_1}{kT}\right). \quad (8)$$

The methanol and water TPD signals (I_{M} and I_{W}) are proportional to the methoxy–OH recombination and the OH combination rates:

$$I_{\mathrm{M}} \propto \frac{\nu}{\beta}\theta_{\mathrm{M}}\theta_{\mathrm{OH}}\exp\left(-\frac{E_1}{kT}\right) \quad (9)$$

$$I_{\mathrm{W}} \propto \frac{\nu}{\beta}\theta_{\mathrm{OH}}^2\exp\left(-\frac{E_2}{kT}\right) \quad (10)$$

We assume that for temperatures safely below the desorption temperature all defect sites are covered with methoxy groups, therefore we set $\theta_{\mathrm{M}}(100\ \mathrm{K}) = \theta_{\mathrm{OH}}(100\ \mathrm{K}) = 0.075$. The methoxy and OH coverages are calculated as function of temperature by numerically solving the differential eqn (7) and (8). A good agreement with the experimentally observed desorption temperature is obtained for $E_1 = E_2 = 0.75$ eV per molecule.

Fig. 8(a) shows the calculated methoxy and hydroxyl coverage as a function of temperature, whereas panel (b) displays the calculated TPD signals for methanol and water. After complete OH loss, the methoxy coverage stabilises at approximately half of the initial coverage, which is in reasonable agreement with the experimental results: according to XPS (see Fig. 6) the methoxy coverage at 230 K is about 2-times as high as at 350 K. We note that in our model the peak temperatures of the calculated methanol and water peak are approximately equal. This implies that for the measured spectrum in Fig. 5 the mass 18 peak resulting from water formed by the combination reaction of hydroxyl groups overlaps with the mass 18 peak originating from the exchange reaction of desorbing methanol in the mass spectrometer housing. The weak water desorption signal between 230 K and 300 K thus probably also contains a contribution of water formed *via* reaction of hydroxyl groups.

The energy barriers for methoxy–OH recombination and OH–OH group combination are 0.1 eV lower for LT adsorption (obtained *via* modelling the temperature of recombinative methanol desorption of a low temperature methanol adsorbate) than for RT adsorption (obtained *via* modelling of the data

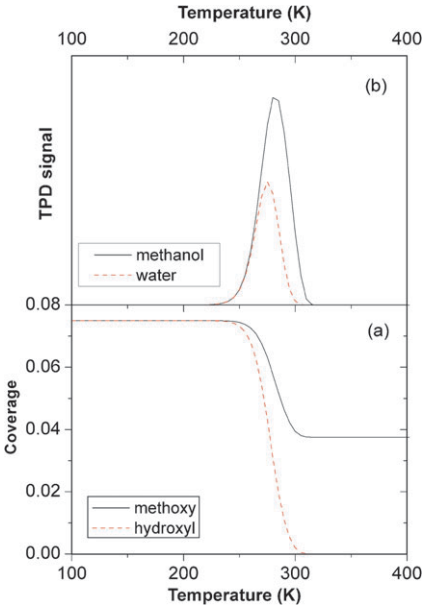

Fig. 8 (a) Calculated methoxy coverage (solid line) and OH coverage (dashed line) *versus* temperature for a model that includes the recombination of methoxy and OH and the simultaneous combination of OH groups. The corresponding calculated TPD signals for methanol (solid line) and water (dashed line) are plotted in (b).

presented in Fig. 7(b)). In view of the assumptions and simplifications of the used models, we feel that the agreement is quite reasonable. Apart from simplifications like neglecting the influence of diffusion and the use of a fixed attempt frequency of 10^{13} s^{-1}, possible coverage-dependences of the energy barriers and the attempt frequencies were both not included. Another possible error source is the presence of different types of surface defects (single, double, triple, *etc*), which may exhibit different reactivies and thus would need to be considered independently in eqn (4) and (5). However, in view of the limited number of data points and the noise of the data we feel that this probably would not give reliable results and constrained the calculations to a single activation energy/attempt frequency pair, which would approximately model the most abundant and active type of defect.

3.7 DFT results on methanol adsorption

The experiments show that unreduced $V_2O_5(001)$ interacts only weakly with methanol. DFT calculations with the PBE functional using a 3×1 surface unit cell, yield an adsorption energy of 0.16 eV which supports the experimental result. The energy for the formation of a surface vanadyl oxygen vacancy on $V_2O_5(001)$ is reduced by a strong lattice relaxation effect. For a single defect on a 3×1 surface we obtain 1.84 eV, in good agreement with previous work[31,32] (see also Hermann *et al.*[33] who previously discussed the case of oxygen vacancy formation and water as well as OH desorption from $V_2O_5(001)$). This particularly low defect formation energy is due to the formation of a V–O–V bond to the vanadyl oxygen of the second crystal layer. Hereby, two V^{IV} ions are created, which is preferable to one V^{III} and one V^{V}. The surface vanadium atom retains a fivefold coordination due to the formation of the bond. This also has the consequence that

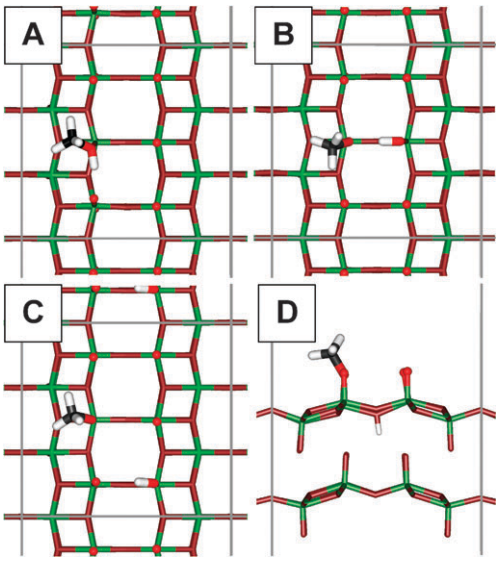

Fig. 9 Calculated structures for methanol adsorption on an isolated defect.

the energy gain upon adsorption is relatively low. DFT yields an adsorption energy of 0.64 eV for molecular methanol bound in the geometry shown in Fig. 9A. A hydrogen bond to the adjacent vanadyl oxygen in the row stabilises the structure. A structure with a hydrogen bond to the vanadyl oxygen at the other side of the double row (*i.e.* across the surface V–O–V bridge) is only 0.01 eV less stable. The energy for dissociative adsorption with the methoxy bound to the vanadium atom at the defect site and the hydrogen atom to a surface oxygen atom depends on the binding site of the hydrogen atom. For the structures shown in Fig. 9B and 9C DFT yields energies of 0.41 and 0.57 eV, respectively. For hydrogen bound to a neighbouring vanadyl oxygen atom in the same row (not shown here) the energy is 0.34 eV. Dissociative adsorption is disfavoured for these structures since the energies are all smaller than the one for molecular adsorption (0.64 eV). However, a structure where the hydrogen atom is located below the surface and binds to a bridging oxygen atom (Fig. 9D) is energetically more stable than a molecular adsorbate. DFT yields an energy of 0.67 eV which is 0.03 eV larger than the energy of molecularly adsorbed methanol.

In the case of water adsorption on a single vanadyl oxygen vacancy molecular adsorption is clearly favoured over dissociative adsorption. The most stable adsorption geometries of molecular water on a single defect and the hydroxyl groups resulting from dissociation of this water molecule are illustrated in Fig. 10A and 10B. The binding energies are 0.64 eV (molecular) and 0.44 eV (dissociated) which means that hydroxyl groups on the surface will react to form water as soon as the temperature is high enough to overcome the energy barriers associated with water formation. The structure shown in Fig. 10B is stabilised by hydrogen bonds between the hydroxyl groups and the vanadyl groups in the opposite rows. A structure where two hydroxyl groups bend towards the same vanadyl group is shown in Fig. 10C. Starting from this structure water could be formed by transfer of hydrogen.

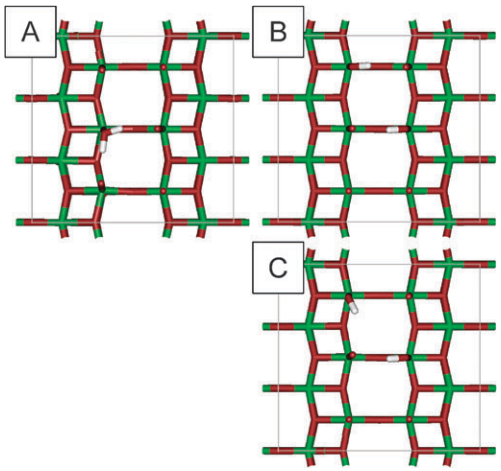

Fig. 10 Calculated structures for water adsorption on an isolated defect.

With a binding energy of 0.36 eV this structure is energetically slightly disfavoured over the structure shown in Fig. 10B.

With the aim of acquiring information regarding the formation of type B double defects the adsorption of molecular and dissociated water near to a vanadyl oxygen vacancy was also studied. Fig. 11A illustrates the structure of water adsorbed on one of the two defects of a type B double defect. The binding energy of this structure is 0.74 eV which is slightly larger than the binding energy of water on a single defect (0.64 eV). After dissociation of the water molecule and transfer of the hydrogen atoms to the neighbouring vanadyl atoms in the same vanadyl row the structure displayed in Fig. 11B results. The energy of the configuration is 0.38 eV. These results do not directly give a clue for the mechanism of the formation of type B defects since the fact that the binding energies are different does not mean that water desorption from a site with a neighbouring defect is preferred over desorption from other sites. However, the results clearly, and not unexpectedly, show that the presence of a defect modifies the adsorption energetics. This will not just apply to binding energies but also to reaction barriers. We assume that the reason for the formation of type B defects is a modified reaction barrier. The hydroxyl groups resulting from methanol dissociation cannot desorb directly; they must react to form water before they can desorb. We assume that the presence of a defect lowers the reaction barrier for water formation such that this reaction is promoted in the vicinity of a defect. After water formation the molecules may desorb, leaving behind a new oxygen vacancy in the geometry of a type B defect. Thus,

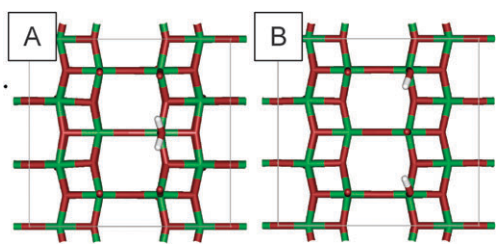

Fig. 11 Calculated structures for water adsorption on a double defect.

single defects would represent catalytic centres for water formation.

4. Summary

The partial oxidation of methanol on V_2O_5(001) films supported on Au(111) was investigated. On non-reduced surfaces methanol adsorbs only in molecular form, consequently no formaldehyde production takes place. On reduced surfaces methanol forms methoxy groups, which react to produce formaldehyde in the temperature range from 400 K to 550 K. Other reaction products were not observed.

Methoxy groups can be stabilised at room temperature only when the surface is free of hydroxyl groups since otherwise methoxy and hydroxyl groups may react to form methanol, which desorbs between 230 and 300 K. Hydroxyl groups can also react with other hydroxyl groups to form water, which probably desorbs in the same temperature regime. If large amounts of methanol are dosed at room temperature, water formation removes all hydroxyl groups from the surface, which finally stabilises a layer of methoxy.

STM images show that the density of surface defects decreases due to methoxy formation, except for pair defects perpendicular to the vanadyl double rows whose density increases upon methanol dosage. We attribute this to the promotion of water formation from hydroxyl groups near to a single defect *via* a reduction of the energy barrier. Water desorption produces another oxygen vacancy so that a vacancy pair results.

Numerical simulations were performed using a kinetic model that includes both the reaction of methoxy and hydroxyl groups to form methanol and the simultaneous combination of OH groups to form water. The results are in good agreement with experimental data for the formaldehyde yield as a function of the methanol dose at 300 K using activation energies of 0.85 eV for methanol and water formation and attempt frequencies of 10^{13} s^{-1}. From a simulation of TPD data, activation energies of 0.75 eV were obtained. These values are considered to be in reasonable agreement in view of the simplifications that were used in the model.

DFT essentially supports the experimental findings. Molecular methanol is only weakly bound to a non-defective vanadyl-terminated V_2O_5(001) surface (E_B = 0.16 eV). The bond to a vanadyl oxygen vacancy is stronger (0.64 eV). Dissociation into surface-bound methoxy and hydrogen is only slightly preferred (0.67 eV, with the hydrogen atom bound to a bridging oxygen atom). Molecular water on a defect has the same binding energy as molecular methanol (0.64) but dissociated water is less strongly bound (0.44 eV). Molecular adsorption on a double defect of type B geometry gives a slightly stronger bond for molecular water (0.74 eV) whereas the energy of the dissociated state is reduced (0.38 eV). We assume that the presence of the defect not only modifies the binding energies but also the reaction barrier for water formation which might be reason for the increase of the density of the type B double defects upon methanol adsorption. However, further theoretical effort would be required to substantiate this hypothesis.

Acknowledgements

This work has been supported by the Deutsche Forschungsgemeinschaft (Sonderforschungsbereich 546, *Transition Metal Oxide Aggregates*), the Fonds der Chemischen Industrie and by a computer time grant at Norddeutscher Verbund für Hoch- and Höchstleistungsrechnen (HLRN).

References

1 G. Deo and I. E. Wachs, *J. Catal.*, 1994, **146**, 323.
2 I. E. Wachs and B. M. Weckhuysen, *Appl. Catal., A*, 1997, **157**, 67.
3 L. J. Burcham and I. E. Wachs, *Catal. Today*, 1999, **49**, 467.
4 Q. Wang and R. J. Madix, *Surf. Sci.*, 2001, **474**, L213.
5 Q. Wang and R. J. Madix, *Surf. Sci.*, 2002, **496**, 51.
6 G. S. Wong, M. R. Concepcion and J. M. Vohs, *J. Phys. Chem. B*, 2002, **106**, 6451.
7 A. Uhl, H. L. Abbott, M. Baron, D. J. Stacchiola, S. Shaikhutdinov and H.-J. Freund, to be published.
8 Y. Romanyshyn, S. Guimond, H. Kuhlenbeck, S. Kaya, R. P. Blum, H. Niehus, S. Shaikhutdinov, V. Simic-Milosevic, N. Nilius, H.-J. Freund, M. V. Ganduglia-Pirovano, R. Fortrie, J. Döbler and J. Sauer, *Top. Catal.*, 2008, **50**, 106.
9 J. Döbler, M. Pritzsche and J. Sauer, *J. Am. Chem. Soc.*, 2005, **127**, 10861.
10 S. Guimond, D. Göbke, Y. Romanyshyn, J. M. Sturm, M. Naschitzki, H. Kuhlenbeck and H.-J. Freund, *J. Phys. Chem. C*, 2008, **112**, 12363.
11 S. Guimond, J. M. Sturm, D. Göbke, Y. Romanyshyn, M. Naschitzki, H. Kuhlenbeck and H.-J. Freund, *J. Phys. Chem. C*, 2008, **112**, 11835.
12 M. Heber and W. Grünert, *J. Phys. Chem. B*, 2000, **104**, 5288.
13 R.-P. Blum, H. Niehus, C. Hucho, R. Fortrie, M. V. Ganduglia-Pirovano, J. Sauer, S. Shaikhutdinov and H.-J. Freund, *Phys. Rev. Lett.*, 2007, **99**, 226103.
14 STM 1, Omicron Nanotechnology, Taunusstein, Germany, http://www.omicron.de.
15 STM images were processed with the free WSxM program, downloadable at http://www.nanotec.es.
16 VG Smart IQ+, http://www.vacgen.com.
17 P. Feulner and D. Menzel, *J. Vac. Sci. Technol.*, 1980, **17**, 662.
18 See http://cms.mpi.univie.ac.at/vasp/.
19 NIST Chemistry WebBook, http://webbook.nist.gov/chemistry.
20 Y. Romanyshyn, S. Guimond, D. Göbke, J. M. Sturm, A. Uhl, H. Kuhlenbeck and H.-J. Freund, to be published.
21 T. Feng and J. M. Vohs, *J. Catal.*, 2004, **221**, 619.
22 K. S. Kim and M. A. Barteau, *Surf. Sci.*, 1989, **223**, 13.
23 H. Idriss, K. S. Kim and M. A. Barteau, *Surf. Sci.*, 1992, **262**, 113.
24 T. R. Dillingham and D. M. Cornelison, *Surf. Sci. Spectra*, 1999, **6**, 146.
25 Ch. Ammon, A. Bayer, G. Held, B. Richter, Th. Schmidt and H.-P. Steinrück, *Surf. Sci.*, 2002, **507–510**, 845.
26 D. R. Mullins, M. D. Robbins and J. Zhou, *Surf. Sci.*, 2006, **600**, 1547.
27 L. J. Burcham and I. E. Wachs, *Catal. Today*, 1999, **49**, 467.
28 M. Abu Haija, S. Guimond, A. Uhl, H. Kuhlenbeck and H.-J. Freund, *Surf. Sci.*, 2006, **600**, 1040.
29 Wolfram Research, http://www.wolfram.com.
30 P. A. Redhead, *Vacuum*, 1962, **12**, 203.
31 M. V. Ganduglia-Pirovano and J. Sauer, *Phys. Rev. B*, 2004, **70**, 045422.
32 J. Sauer and J. Döbler, *Dalton Trans.*, 2004, **19**, 3116.
33 K. Hermann, M. Witko, R. Druzinic and R. Tokarz, *Top. Catal.*, 2000, **11/12**, 67.